

# Soliton creation during a Bose-Einstein condensation

Bogdan Damski and Wojciech H. Zurek

*Theoretical Division, Los Alamos National Laboratory, MS-B213, Los Alamos, NM 87545, USA*

We use stochastic Gross-Pitaevskii equation to study dynamics of Bose-Einstein condensation. We show that cooling into a Bose-Einstein condensate (BEC) can create solitons with density given by the cooling rate and by the critical exponents of the transition. Thus, counting solitons left in its wake should allow one to determine the critical exponents  $z$  and  $\nu$  for a BEC phase transition. The same information can be extracted from two-point correlation functions.

When temperature of a bosonic cloud is lowered, atoms undergo a thermal gas – Bose-Einstein condensate phase transition. Sufficiently slow cooling process creates a condensate in the ground state. Its macroscopic quantum properties have been studied over the last decade. Faster cooling should result in creation of an excited condensate that contains vortices and solitons.

Non-equilibrium condensation is an example of dynamics of phase transitions. Their study started with investigations of topological defect creation in cosmological phase transitions [1]. It was then pointed out that condensed matter systems (superconductors, liquid  $^3\text{He}$  and  $^4\text{He}$ , etc.) can be used to test this cosmological scenario, and that the nature of the transition will determine density of defects [2]. Kibble-Zurek mechanism (KZM) describes how topological defects (vortices, monopoles, kinks, etc.) are created during non-equilibrium second order phase transitions (see [3, 4] for experimental evidence).

Data on spontaneous creation of solitons and vortices during Bose-Einstein condensation are still scarce. Two groups have seen them: the Anderson group observed vortices in a three dimensional trap [4], while the Engels' group reported observation of solitons in a quasi one dimensional (1D) setup that does not support topological defects [5]. Therefore, it is important to understand non-equilibrium dynamics of Bose-Einstein condensation. Moreover, it is also interesting to find out if the KZM, studied theoretically and experimentally in various physical systems [2–4, 6–9], applies to non-topological excitations (e.g., solitons). We propose to kill two birds with one stone by studying dynamics of Bose-Einstein condensation in a quasi-one 1D system.

As the atom cloud is cooled from above the critical point, the system adjusts adiabatically to driving because its relaxation time is initially short. Near the critical point, however, the relaxation time diverges due to critical slowing down. The system goes out of equilibrium before reaching the critical point and approximately freezes out entering the impulse stage of its dynamics. As the condensate forms, its different parts choose to break the symmetry in an uncorrelated way, which results in creation of defects. Their spacing depends on the quench rate given by the rate of temperature change [2]: the slower we go, the more adiabatic the evolution is, and

so the larger the separation between the defects will be. The transition from adiabatic to impulse regime happens when the relaxation time  $\tau$  becomes comparable to the quench rate  $\varepsilon/\dot{\varepsilon}$  ( $\varepsilon$  is the distance from the critical point):

$$\tau(\varepsilon(t)) = \left| \frac{\varepsilon}{\dot{\varepsilon}} \right|. \quad (1)$$

Assuming a linear quench, i.e.,  $|\dot{\varepsilon}| = \tau_Q^{-1}$ , where  $\tau_Q$  is the quench timescale, the system goes out of equilibrium at

$$\hat{\varepsilon} \sim \tau_Q^{\frac{-1}{1+z\nu}}. \quad (2)$$

This imprints a characteristic time scale  $\hat{t} = \tau_Q \hat{\varepsilon} = \tau_Q^{z\nu/(1+z\nu)}$  onto the system, so that defect density depends on time through  $t/\hat{t}$  or equivalently  $\varepsilon(t)/\hat{\varepsilon}$ . The typical distance between defects scales as

$$\hat{\xi} = \xi(\hat{\varepsilon}) \sim \tau_Q^{\frac{\nu}{1+z\nu}}, \quad (3)$$

in the KZM freeze out picture [2]. Above  $z$  and  $\nu$  are the critical exponents defining the equilibrium coherence length  $\xi$  and relaxation timescale  $\tau$ :

$$\xi \sim |\varepsilon|^{-\nu}, \quad \tau \sim |\varepsilon|^{-z\nu}. \quad (4)$$

Thus, KZM (presented above) proposes a way to extract essential features of the non-equilibrium phase transition dynamics from equilibrium critical behavior of a system.

The exact simulation of Bose-Einstein condensation is extremely involved (if at all possible) [10]. We restrict ourselves to a tractable model: the stochastic Gross-Pitaevskii equation (SGPE) that has been successfully applied to studies of Bose-Einstein condensates lately [10]. Our calculations provide the first numerical results on dynamics of soliton production in the course of second order phase transitions, and extend the KZM to non-topological excitations. Former studies of 1D models, driven across a critical point, were focused on systems supporting topological defects (e.g., kinks [8]).

Stochastic Gross-Pitaevskii equation reads [11]:

$$(i - \gamma)\partial_t \phi = -\frac{1}{2}\partial_x^2 \phi + \varepsilon \phi + g|\phi|^2 \phi + \vartheta(x, t), \quad (5)$$

where noise, coming from a thermal cloud, satisfies

$$\langle \vartheta(x, t) \vartheta^*(x', t') \rangle = 2\gamma T \delta(x - x') \delta(t - t'). \quad (6)$$

Above  $\gamma$  represents damping coming from thermal cloud – condensate interactions,  $T$  is the thermal cloud temperature, and  $\varepsilon = -\mu$ , where  $\mu$  is the chemical potential.

Forgetting for a while about damping and noise we see that the system is described by the energy functional

$$\mathcal{E} = \int dx \frac{1}{2} |\partial_x \phi|^2 + V(|\phi|), \quad V(|\phi|) = \varepsilon |\phi|^2 + \frac{g}{2} |\phi|^4. \quad (7)$$

For  $\varepsilon > 0$  ( $\mu < 0$ ) the minimum of  $V(|\phi|)$  corresponds to  $\phi = 0$ : order parameter vanishes above condensation temperature, and the system is in the symmetric phase. When  $\varepsilon < 0$  ( $\mu > 0$ ) there is a minimum of  $V(|\phi|)$  at  $|\phi|^2 = -\frac{\varepsilon}{g}$ , and the system is in the broken-symmetry phase where  $\phi = \sqrt{-\varepsilon/g} \exp(i\theta)$ : a condensate forms.

We quench the system from the symmetric to the broken-symmetry phase. The phase  $\theta$  will not be chosen uniformly in the broken-symmetry phase because the quench freezes a characteristic coherence length,  $\hat{\xi}$ , when the system goes out of equilibrium on the symmetric side. This leads to phase gradients that seed soliton-like density notches around which the phase of the order parameter changes abruptly [12, 13].

For simplicity, we model cooling of a bosonic gas by assuming that chemical potential grows across the critical point, while damping  $\gamma$  and noise correlations remain constant. This approximation is motivated by the fact that defect production takes place near the critical point, where chemical potential changes drive the transition influencing dynamics most, while the variations in  $\gamma$  and noise correlators are of secondary importance.

In the following we need freeze out values of  $\hat{\varepsilon}$  and  $\hat{\xi}$ . As  $z = 2$  and  $\nu = 1/2$  for SGPE, Eqs. (2) and (3) imply

$$\hat{\varepsilon} \sim \tau_Q^{-1/2}, \quad \hat{\xi} \sim \tau_Q^{1/4}. \quad (8)$$

We drive the system from the symmetric phase to the broken-symmetry phase at a constant rate:

$$\varepsilon(t) = -\frac{t}{\tau_Q}, \quad (9)$$

where  $t = -\varepsilon_0 \tau_Q \rightarrow \varepsilon_0 \tau_Q$ . The evolution starts away from the critical point at  $\varepsilon = \varepsilon_0 \gg 1$ . The system passes through the critical point at  $\varepsilon, t = 0$ , and ends its evolution far away from the critical point at  $\varepsilon = -\varepsilon_0$ .

The discussion of KZM can be analytically illustrated in our model on the symmetric side. After dropping the nonlinear term we are left with Langevin-type equation:

$$(i - \gamma) \partial_t \phi = -\frac{1}{2} \partial_x^2 \phi + \varepsilon \phi + \vartheta(x, t). \quad (10)$$

This equation can be solved exactly providing the following relaxation time and coherence length *in equilibrium*:

$$\tau = \frac{1 + \gamma^2}{\gamma} \frac{1}{\varepsilon}, \quad \xi = \frac{1}{\sqrt{2}} \frac{1}{\sqrt{\varepsilon}}, \quad (11)$$

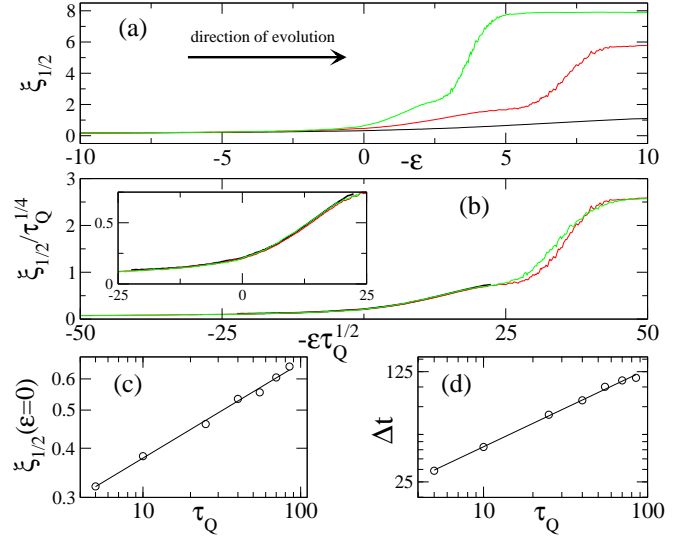


FIG. 1: Half-width of the averaged two-point correlation function (15) during the quench:  $\xi_{1/2}$ . **(a) and (b)**:  $\xi_{1/2}$  before and after rescalings. On both plots black, red, and green lines correspond to  $\tau_Q = 5, 25$  and  $85$ , respectively. The inset magnifies the region where the KZM works best. **(c)** Illustration that quench imprints a characteristic length scale  $\hat{\xi} \sim \tau_Q^{\nu/(1+z\nu)} = \tau_Q^{1/4}$  (8). We study  $\xi_{1/2}$  at the critical point. The scale is logarithmic on both axes: circles show numerics, while the straight line is a fit to numerics:  $\ln \xi_{1/2}(\varepsilon = 0) = -1.53 \pm 0.03 + (0.24 \pm 0.01) \ln \tau_Q$ . The fit confirms the predicted  $1/4$  exponent. **(d)** Illustration that quench imprints a characteristic time scale  $\hat{t} \sim \tau_Q^{z\nu/(1+z\nu)} = \tau_Q^{1/2}$ . We study time  $\Delta t$  passing from entering the broken-symmetry phase to the moment when  $\xi_{1/2}/\hat{\xi}$  reaches a threshold, assumed here to be  $0.5$ , i.e., to be near the center of the region where rescalings work on the broken-symmetry side [see inset of Fig. (b)]. The scale is logarithmic on both axes: circles show numerics, while straight line is a fit to numerics:  $\ln \Delta t = 2.60 \pm 0.04 + (0.49 \pm 0.01) \ln \tau_Q$ . This is in good agreement with theoretical prediction of  $\Delta t \sim \tau_Q^{1/2}$ . We use for this plot  $\hat{\xi}$  taken from the fit done in plot (c):  $\hat{\xi} = \tau_Q^{0.24}$ . Fits from plots (c) and (d) allow for measurement of  $z$  and  $\nu$  critical exponents. All results presented above are averages over 100 runs with different noise. See [14] for other parameters.

respectively. It implies  $z = 2$  and  $\nu = 1/2$ . We obtained (11) by studying the two point correlation function

$$C(x, t|x', t') = \langle \phi(x, t) \phi^*(x', t') \rangle - \langle \phi(x, t) \rangle \langle \phi^*(x', t') \rangle, \quad (12)$$

where  $\langle \dots \rangle$  denotes averaging over different noise realizations. We found that  $C(x, t|x', t)$  decays on the length scale  $\xi$  while  $C(x, t|x, t')$  decays on the timescale  $\tau$ .

Solving (1) with (9) and (11) we determine that the adiabatic - impulse border is at

$$\hat{\varepsilon} = \sqrt{\frac{1 + \gamma^2}{\gamma}} \frac{1}{\sqrt{\tau_Q}},$$

so the system “freezes” when its coherence length equals

$$\hat{\xi} = \xi(\hat{\varepsilon}) = \frac{1}{\sqrt{2}} \left( \frac{\gamma}{1 + \gamma^2} \right)^{1/4} \tau_Q^{1/4}.$$

Assuming for simplicity that  $\varepsilon_0 \rightarrow \infty$ , and solving analytically (10) with (9) we find that far away from the critical point the system follows adiabatically the instantaneous equilibrium solution

$$C(x, t|x', t) = \frac{T}{\sqrt{2\varepsilon(t)}} \exp\left(-|x - x'| \sqrt{2\varepsilon(t)}\right). \quad (13)$$

Near the critical point, i.e., when  $\varepsilon \lesssim \hat{\varepsilon}$  we have to refer to the exact solution that reads

$$C(x, t|x', t) = \langle |\phi(\hat{\varepsilon})|^2 \rangle_{eq} f(|x - x'|/\hat{\xi}, \varepsilon(t)/\hat{\varepsilon}), \quad (14)$$

where  $f(a, b) = \frac{1}{\sqrt{\pi}} \int dk \cos(ka) \exp((b + k^2)^2) \text{erfc}(b + k^2)$ ,  $\langle \dots \rangle_{eq}$  denotes equilibrium averaging, and  $\langle |\phi(\hat{\varepsilon})|^2 \rangle_{eq} = T/\sqrt{2\hat{\varepsilon}}$ . Naturally, (14) reduces to (13) for  $\varepsilon \gg \hat{\varepsilon}$ .

The result (14) shows that correlations are induced on the length scale  $\hat{\xi}$ , which is given by the correlation length at the border between adiabatic and impulse regimes. Another interesting feature of (14) is that it scales as  $\tau_Q^{1/4}$ : the equilibrium correlations (13) calculated at  $\varepsilon(t) = \hat{\varepsilon}$  scale in the same way. Similarly, there is a freeze out time scale  $\hat{t}$  imprinted into system's dynamics through the relation  $\varepsilon(t)/\hat{\varepsilon} = t/\hat{t}$ . All these results are in perfect agreement with KZM.

On the broken-symmetry side we rely on numerics. As above, we test our theory by looking at the characteristic length and time scales imprinted onto the system by the quench. This is done by studying half-width of the averaged two-point correlation function, i.e.,

$$\frac{1}{l} \int_0^l dx |C(x, t|x + r, t)|, \quad (15)$$

where the averaging over the system size  $l$  is applied. Fig. 1 shows that in whole symmetric phase, as well as in the broken-symmetry phase for  $-\varepsilon\tau_Q^{1/2} \lesssim 25$ , the following scaling works very well

$$\xi_{1/2} \sim \hat{\xi} f(\varepsilon/\hat{\varepsilon}) \sim \tau_Q^{\frac{\nu}{1+z\nu}} f\left(\varepsilon\tau_Q^{\frac{1}{1+z\nu}}\right) = \tau_Q^{1/4} f\left(\varepsilon\tau_Q^{1/2}\right). \quad (16)$$

Scaling (16) is in perfect agreement with KZM and allows for measurement of critical exponents  $z$  and  $\nu$  (see Fig. 1). We use here SGPE mean-field exponents ( $z = 2$  and  $\nu = 1/2$ ) to compare our numerics to theory. In an actual experiment, however, other values of critical exponents may be relevant (see [15] and references cited therein). Indeed, critical exponents can be experimentally studied, for example, with the help of cavity-assisted cold atom counting recently explored in the Esslinger's group at ETH Zurich [15]. There, the

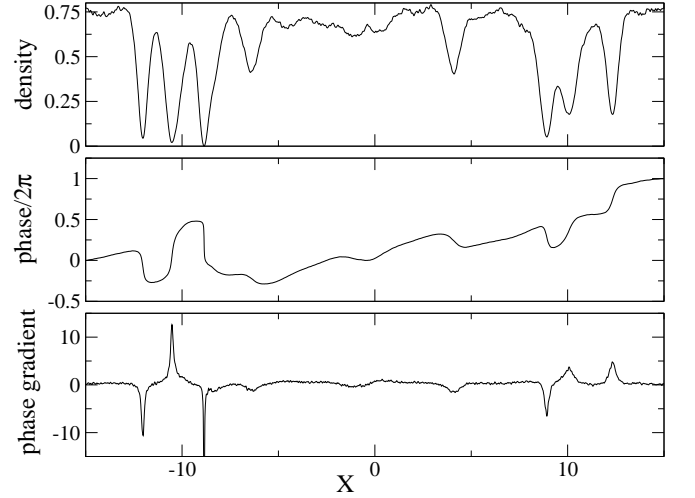


FIG. 2: Snapshot of density  $|\phi(x)|^2$ , phase  $\arg(\phi)$ , and gradient of phase  $\frac{d}{dx}\arg(\phi)$  (the velocity field). The snapshot is taken for one evolution (no averaging) at  $\varepsilon(t) = 10$  for  $\tau_Q = 10$ . See [14] for other parameters.

system was near equilibrium and so the study of two-point correlation functions was aimed at determination of the critical exponent  $\nu$ . Nonequilibrium version of this experiment can provide a new way for measurement of the exponent  $\nu$  and can reveal the dynamical exponent  $z$ . All this is possible due to presence of the characteristic length scale  $\xi_{1/2}$  in the non-equilibrium state of the condensate. The most striking consequence of existence of this length scale is the creation of solitons.

Qualitatively, we observe soliton-like solutions in the broken-symmetry phase: see Fig. 2. There are several deep density notches there, and the phase of the order parameter changes steeply around them. These are typical signatures of solitons [12]. They are in qualitative agreement with Engels' experiments studying density profiles after the condensation process [5].

Quantitatively, we would like to find out if the critical scalings (4) can be retrieved from soliton counting. This is of both fundamental and practical interest: soliton counting can be significantly easier than measurement of the correlation functions. The typical number of solitons shall be inversely proportional to the size of correlated domains that have chosen to break the symmetry in the same way: phase jumps between the domains provide seeds for solitons. Thus, we predict

$$\# \text{ of solitons} \sim \xi_{1/2}^{-1} \sim \tau_Q^{\frac{\nu}{1+z\nu}} \tilde{f}\left(\varepsilon\tau_Q^{\frac{1}{1+z\nu}}\right) = \tau_Q^{-1/4} \tilde{f}\left(\varepsilon\tau_Q^{1/2}\right). \quad (17)$$

We count solitons by fitting the solitonic solution of the Gross-Pitaevskii equation (no noise/damping) around every minimum of the density  $|\phi|^2$ :

$$n_{min} + (n_0 - n_{min}) \tanh^2[(x - x_0)\sqrt{g(n_0 - n_{min})}].$$

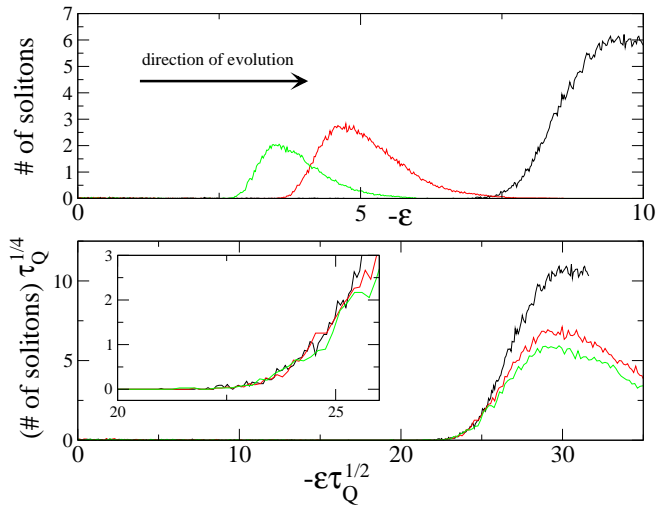


FIG. 3: Number of solitons in the broken-symmetry phase before and after rescalings. On both plots black, red and green lines correspond to  $\tau_Q = 10, 40$  and  $70$ , respectively. The inset magnifies the region where KZM works best. The results present average over 100 runs with different noise. See [14] for other parameters.

We use only modulus of the order parameter as it is typically the only quantity measurable in a standard BEC setup. The fit gives the three parameters of the soliton solution: position ( $x_0$ ), minimum density ( $n_{min}$ ), and background density ( $n_0$ ). The latter two are related to soliton and sound velocities, respectively. We then compare the fitted depth of the soliton,  $n_0 - n_{min}$ , to the numerical data. When the two do not differ by more than 50%, we count the density minimum as a soliton. We have checked that the same conclusions are obtained for other reasonable thresholds between 30% and 60%. The outcome of this procedure is presented in Fig. 3, where the number of solitons for  $-\varepsilon\tau_Q^{1/2} \lesssim 25$  follows closely (17) in agreement with KZM and our studies of the width of the two-point correlation functions. The drawback with respect to the latter is that solitons need some time to develop before they can be counted, thus their macroscopic number can be observed in a narrow window of  $20 \lesssim -\varepsilon\tau_Q^{1/2} \lesssim 25$ . Another complication is that solitons are more vulnerable to damping than two-point correlation function: damping removes solitons from the system by decreasing their depth. This shall not be a problem with an actual experiment as there is negligible damping/noise by the end of condensation [13].

Our results were obtained for atoms in a quasi-1D *homogeneous* configuration that can be experimentally realized [16]. In harmonic traps with cigar-shaped BEC's homogeneous scalings would be modified by causality-related considerations [17]. In either case, the experimental data will shed light on the real critical exponents of the cold atom system and facilitate the first experimental determination of the dynamical, i.e.,  $z$  exponent

of the interacting Bose-Einstein condensate.

Summarizing, we have shown that two-point correlation functions after non-equilibrium quench encode critical exponents of the system. We have also predicted that non-equilibrium condensation results in creation of soliton-like excitations whose number depends on a quench rate via the critical exponents. Our results can be “inverted” and used for the experimental determination of the critical exponents for the normal gas – Bose-Einstein condensate phase transition.

We are grateful to Peter Engels for showing us his unpublished experimental data and for stimulating discussions. We thank Ashton Bradley for his very useful comments. We acknowledge the support of the U.S. Department of Energy through the LANL/LDRD Program.

- 
- [1] T.W.B. Kibble, J. Phys. A **9**, 1387 (1976); Phys. Rep. **67**, 183 (1980).
  - [2] W.H. Zurek, Nature (London) **317**, 505 (1985); Acta Phys. Pol. B **24**, 1301 (1993); Phys. Rep. **276**, 177 (1996).
  - [3] I. Chuang *et al.*, Science **251**, 1336 (1991); M.J. Bowick *et al.*, *ibid.* **263**, 943 (1994); C. Bauerle *et al.*, Nature (London) **382**, 332 (1996); V.M.H. Ruutu *et al.*, *ibid.* **382**, 334 (1996); A. Maniv, E. Polturak, and G. Koren, Phys. Rev. Lett. **91**, 197001 (2003); R. Monaco *et al.*, *ibid.* **96**, 180604 (2006).
  - [4] C.N. Weiler *et al.*, Nature **455**, 948 (2008).
  - [5] P. Engels, “Nonlinear Dynamics in BECs: Faraday waves, solitons and quantum shock”, talk at Los Alamos National Laboratory given on 03/06/2008.
  - [6] T.W.B. Kibble, Physics Today **60**, 47 (2007).
  - [7] J. Dziarmaga, arXiv:0912.4034 (2009).
  - [8] P. Laguna and W.H. Zurek, Phys. Rev. Lett. **78**, 2519 (1997); Phys. Rev. D **58**, 085021 (1998).
  - [9] L.E. Sadler *et al.*, Nature (London) **443**, 312 (2006).
  - [10] P.B. Blakie *et al.*, Adv. Phys. **57**, 363 (2008); S. P. Cockburn and N. P. Proukakis, Laser Phys. **19**, 558 (2009).
  - [11] The rescaling  $t \rightarrow t(1+\gamma^2)$  transforms (5) to a canonical form of the SGPE:  $i\partial_t\phi = (1-i\gamma)(-\frac{1}{2}\partial_x^2 + g|\phi|^2 - \mu)\phi + \eta$ , where chemical potential  $\mu = -\varepsilon$  and noise  $\eta$  has the same correlator as in (6). See [10] for review of SGPE.
  - [12] C.J. Pethick and H. Smith, Bose-Einstein condensation in dilute gases (Cambridge University Press, Cambridge UK, 2002).
  - [13] C. Becker *et al.*, Nature Phys. **4**, 496 (2008).
  - [14] In all our simulations we use the following dimensionless parameters:  $\gamma = 10^{-2}$ ,  $T = 5 \times 10^{-4}$ ,  $g = 10$ ,  $\varepsilon_0 = 10$ . The system size is  $l = 30$ . We assume periodic boundary conditions. The noise is generated by randomly choosing  $\text{Re}\vartheta(x,t), \text{Im}\vartheta(x,t) \in [-\alpha, \alpha]$  with uniform probability. There  $2\gamma T = 2\alpha^2\Delta x\Delta t/3$  and  $\Delta x$  is the grid spacing of our simulations ( $l/4096$ ), while  $\Delta t$  is the time step for noise generation ( $2 \times 10^{-3}$ ). The value of  $\gamma$  is consistent with former studies: see e.g. S. Choi, S.A. Morgan and K. Burnett, Phys. Rev. A **57**, 4057 (1998).
  - [15] T. Donner *et al.*, Science **315**, 1556 (2007).
  - [16] T.P. Meyrath *et al.*, Phys. Rev. A **71**, 041604(R) (2005).
  - [17] W.H. Zurek, Phys. Rev. Lett. **102**, 105702 (2009).